Laser-ignited glow discharge in lithium vapor

H. Skenderović,* I. Labazan, S. Milošević, and G. Pichler
Institute of Physics, P.O. Box 304, HR-10000 Zagreb, Croatia
(Received 9 March 2000; published 12 October 2000)

Ignition of lithium glow discharge below self-breakdown voltage is studied for three cases of laser excitation of lithium vapor: the quasiresonant line at 460.3 nm ($2p \rightarrow 4d$), the two-photon resonant line at 639.1 nm ($2s \rightarrow 3d$ transition), or the first resonance at 670.8 nm ($2s \rightarrow 2p$ transition). The conditions for laser ignition of the discharge are described. The differences between the self-breakdown voltage and the breakdown voltage for laser initiation of the discharge are given for different lithium number densities.

PACS number(s): 34.80.Kw, 52.80.−s, 39.30.+w, 52.50.Jm

I. INTRODUCTION

A coupling of light with an electrical discharge is studied in optogalvanic experiments (reviewed in Ref. [1]) where the light is usually a small perturbation. A more dramatic influence of laser light on a discharge is exhibited in laser guiding experiments (Ref. [2] and references therein) where the laser beam is employed for creating a plasma channel.

At total pressure around 1 Torr, a glow discharge [3] is characterized by relatively high voltage (several hundreds of volts at the interelectrode distance of some tens of cm) and modest currents (from a few up to several hundred mA). The voltage across electrodes necessary for the ignition of a normal glow discharge is called the self-breakdown voltage. The voltage necessary to sustain a stable glow discharge is lower than the self-breakdown voltage with the current limited by a resistor in series with the discharge. The voltage stays constant as the current is increased for the discharge in the ''normal'' regime, but it increases for the discharge in the ''abnormal'' regime [3].

There is a long history of studies concerning laser excitation and ionization of alkali-metal vapors [4]. The absorption of laser photons in alkali-metal vapor is possible by tuning the laser frequency to the resonant transition (e.g., $2s \rightarrow 2p$ in lithium), quasiresonant transitions ($2p \rightarrow 3d$, $4d \ldots, 3s, 4s \ldots$ in lithium), and two-photon resonant transitions ($2s \rightarrow 3d, 4d \ldots, 3s, 4s, \ldots$ in lithium).

The efficient ionization of a dense alkali-metal vapor by resonant laser light was first reported by Lucatorto and McIlrath [5]. In their experiment, almost 100% ionization of sodium vapor was produced using 500 ns laser pulses tuned to the sodium $\lambda = 589.6$ nm, $3s_{1/2} \rightarrow 3p_{1/2}$ transition. That interesting effect was further investigated by Tam and Happer [6,7] in Cs vapor with extension of the technique to the cw laser quasiresonant excitation $6p \rightarrow 8d$ at 601 nm. The laser-induced fluorescence from a dense Cs vapor showed recombination continua and plasma-broadened atomic lines [6]. In the process of quasiresonant excitation the role of alkali-metal dimers is recognized to be important [7,8]. Experiments on laser-induced plasmas in alkali-metal vapors have been reviewed in papers by Bahns *et al.* [9] and by Stwalley and Bahns [10].

The theoretical evaluation of laser ionization by resonant light was made by Measures and co-workers [11,12]. In their model, called LIBORS (light ionization based on resonance saturation), the laser rapidly saturates the resonant level. Once the large pool of atoms in resonant state is created, seed electrons are generated by multiphoton ionization from the resonance level, by associative ionization, by laser-induced Penning ionization, and by other ionization processes [12]. Free electrons rapidly gain energy through superelastic collisions with excited atoms so that electron-impact ionization from the resonant level and of collisionally populated upper levels contribute to the rate of ionization together with the single-photon ionization from those upper levels. Almost complete ionization of the excited atoms occurs when a critical electron density is achieved. In the LIBORS scheme, it is important to note that to generate the complete ionization, the critical atom density and relatively long laser pulse (or cw regime) are necessary.

Laser induced ionization can occur also in vapors irradiated by nanosecond laser pulses [13,14] when the ionization is only partial and does not exceed a few percent. In a theoretical approach to ionization of sodium vapor by 10 ns resonant laser pulses in Ref. [14], the LIBORS model is amended by adding energy pooling [15] and Penning ionization processes into the ionization scheme. The spectroscopic observations of laser-produced plasmas in alkali-metal vapors induced by two-photon resonances using a 10 ns pulsed laser have also been reported [16]. The diffuse bands [17] and the atomic lines from the high-lying levels that were present in the fluorescent spectra confirmed the laser ionization of the vapor [16].

Laser-induced ionization in the presence of a static electric field can initiate an electric discharge. The group of Tamura performed several experiments [18–20], involving laser initiation of an electrical discharge in cesium-argon and sodium-argon mixtures. In the first experiment, a XeCl excimer laser was used for one-photon ionization of cesium atoms [18]. The minimum energy of the pulse that could initiate the discharge was 20 mJ. In the second experiment, a dye laser tuned to the sodium resonance line was used [19]. In the third experiment, a long pulse (1.2 μs) high-power laser (8 MW/cm^2) was tuned to the second resonance line (455.5 nm) of the cesium atom [20] and initiated a channel discharge of 60 cm length.

In this paper we report the employment of a 20-ns-long

*FAX: 00 385 1 4680 399. Email address: hrvoje@ifs.hr

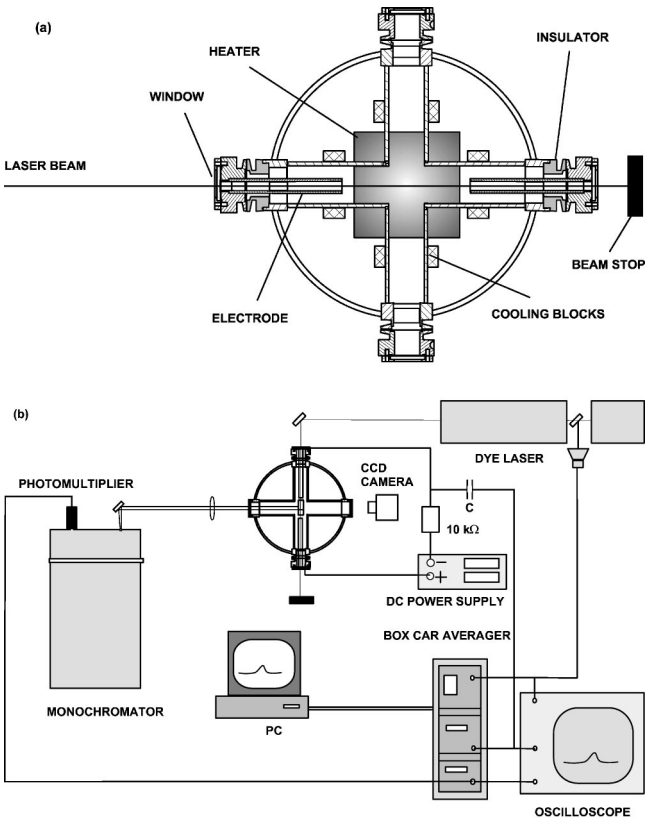

FIG. 1. (a) The modified heat-pipe oven for discharge studies. (b) Experimental setup for laser-induced fluorescence, optogalvanic, and laser-ignition measurements.

laser pulse for ignition of a glow discharge in lithium vapor contained in a modified heat-pipe oven with a specific voltage between the electrodes. The paper is organized as follows. Experimental details are presented in Sec. II. We summarize and discuss various laser ionization processes involved in three ionization cases in Sec. III. Section IV describes experiments with laser ignition of the discharge. Finally, our conclusions are presented in Sec. V.

II. EXPERIMENTAL DETAILS

The crossed heat-pipe oven (HPO), see Fig. 1(a), modified for the discharge studies is made of a stainless-steel tube 3.4 cm in diameter and with 2-mm-thick walls [21]. Hollow stainless-steel electrodes, with inner and outer diameter 8 and 10 mm, allow for passing a laser beam. The interelectrode distance is 16.5 cm. Electrodes can be easily dismounted for the cleaning. The mesh structure on the inner surface of the HPO in the central part acts as a wick in all four arms. The HPO is filled with lithium through one arm under the constant flow of argon. When an external heater heats the central part, a vapor zone of about 8 cm in length is formed within the central part. Upon applying voltage equal to or larger than the self-breakdown voltage between the electrodes, the normal glow discharge is established with positive column plasma made out of hot metal vapor in the heated zone of the HPO. The side-on emission from the positive column may be easily observed through an electrodeless

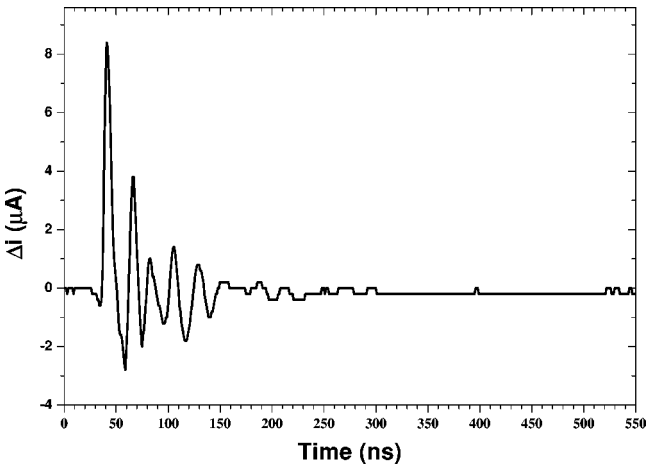

FIG. 2. Time evolution of the OG signal at two-photon resonant transition $2s \rightarrow 3d$. Density of lithium atoms is 5.7×10^{15} cm^{-3} and current through the discharge is 30 mA. Negative current change in the graph represents increase of the current through the discharge.

side arm of the HPO. The temperature of HPO is measured by an Alumel-Chromel thermocouple placed in the heating block. The lithium partial pressure is determined from a tabulated lithium vapor pressure curve [22].

The experimental setup is shown in Fig. 1(b). A stabilized dc power supply is used for setting the voltage and maintaining the discharge. A current limiting resistor (10 kΩ) is placed in series with the HPO discharge. A blocking capacitor (C) for monitoring the optogalvanic (OG) signal is also placed in the electrical circuit, Fig. 1(b).

The laser beam from a pulsed dye laser (LPD 3002E Lambda Physik) pumped by a Xe-Cl excimer laser (LPX 105E Lambda Physik) is used for ignition, OG, and fluorescent measurements. The pulse half-width is about 20 ns and the repetition rate can be varied from 1 to 10 Hz. The typical energy of a single pulse is 2 mJ with a 0.2 cm^{-1} linewidth. Coumarin 102 dye is used for the excitation at quasiresonant transition $2p \rightarrow 4d$ in the lithium atom, and Rhodamin 101 for the two-photon $2s \rightarrow 3d$ transition and resonant $2s \rightarrow 2p$ transition. The laser beam is directed through the hollow electrodes in the HPO in both the laser ignition and laser-induced fluorescence experiments. It is weakly focused in the middle of the heat-pipe oven, between the electrodes. The lithium number density was varied in the range from 10^{14} to 10^{16} cm^{-3}, whereas the total pressure of lithium vapor and the buffer gas (helium) was kept at 2.5 Torr. In front of one of the HPO arms, see Fig. 1(b), a CCD camera is placed for observing the discharge [23].

A typical time evolution of the OG signal obtained from the oscilloscope is shown in Fig. 2. It represents a change in current through the discharge upon the two-photon excitation of a Li atom at $2s \rightarrow 3d$ transition. The density of lithium atoms is 5.7×10^{15} cm^{-3}, and current through the discharge is 30 mA. The shape of the OG signal reveals that the perturbed discharge returns to its stable state by damped plasma current oscillations.

A wavelength-selective excitation spectrum is obtained by setting the monochromator, at a specific wavelength while

scanning the laser wavelength. The laser-induced fluorescence spectrum is obtained by scanning the monochromator at the fixed laser wavelength.

III. LASER IONIZATION IN LITHIUM

The laser light was tuned to one of the following resonances in lithium vapor, Figs. 3(a)–3(c): (a) quasiresonance (QR), $2p \rightarrow 4d$, at 460.3 nm; (b) two-photon resonance (TPR), $2s \rightarrow 3d$, at 639.1 nm; and (c) first resonance (FR), $2s \rightarrow 2p$, at 670.8 nm.

The most probable processes that could generate ions are tabulated in Table I. Numbers of absorbed photons needed for each ionization process are given in parentheses at the end of each cycle.

Although these processes are well known from the literature, we performed here additional LIF and OG studies to clarify their role in the ionization of lithium vapor under the conditions of the present experiment.

A. $2p \rightarrow 4d$ quasiresonance

The case of QR ionization appears to follow the most complicated schemes which proceed either through a dimer-atomic absorption path or dimer two-step absorption [see Fig. 3(a) and processes enumerated in Table I].

In the first scheme, a laser photon excites the dimer to the $Li_2\ B\,^1\Pi_u$ state, which corresponds to the $2s+2p$ asymptote:

$$Li_2(X) + h\nu_{460} \rightarrow Li_2(B). \tag{1}$$

At our experimental conditions, transitions to continuum levels of the $B\,^1\Pi_u$ state contribute about 10% to the total absorption [24]. These transitions directly produce $Li(2p)$ atoms. The energy from bound excited dimers is transferred to atoms either through collisional dissociation,

$$Li_2(B) + M \rightarrow Li(2p) + Li(2s) + M, \tag{2}$$

or molecule-atom energy transfer,

$$Li_2(B) + Li(2s) \rightarrow Li_2(X) + Li(2p). \tag{3}$$

The second photon from the same laser pulse excites the $4d$ level, from which associative ionization or photoionization is possible:

$$Li(2p) + h\nu_{460} \rightarrow Li(4d), \tag{4}$$

$$Li(4d) + Li(2s) \rightarrow Li_2^+ + e^-, \tag{5}$$

$$Li(4d) + h\nu_{460} \rightarrow Li^+ + e^-. \tag{6}$$

The second scheme represents photoionization of the $Li_2\ B\,^1\Pi_u$ state,

$$Li_2(B) + h\nu_{460} \rightarrow Li_2^+ + e^-. \tag{7}$$

Process (7) pertains for a wavelength interval around 460.3 nm. The long-wavelength limit to the two-photon ionization of lithium atom is at 459.8 nm, but two-photon ionization from the ground state is quite weak [25].

For illustration we show in Fig. 4 an excitation spectrum monitoring the $3d \rightarrow 2s$ transition at 610.3 nm with a lithium number density of 1.2×10^{15} cm^{-3}. There is a strong signal at the position of the quasiresonant line at 460.3 nm. The background originates from molecular absorption to the $Li_2\ B\,^1\Pi_u$ state. The strong signal at 460.3 nm is the result of direct pumping at the $2p \rightarrow 4d$ transition that is followed by (a) collisional redistribution of population among $4l$ levels and radiative decays $4f \rightarrow 3d$ and $4p \rightarrow 3d$, or (b) radiative decay $4d \rightarrow 3p$ and collisional population of the $3d$ level. The OG excitation spectrum taken at a 30 mA current is also shown in Fig. 4. The excitation signal shows that there is a significant population of the $Li(4d)$ state created due to the laser pulse at the position of the QR. But, once the $Li(4d)$ state is populated it decays to lower states, as described above, before the associative ionization (5) or photoionization (6) takes place. That is the reason why the OG signal does not show enhancement at the quasiresonance. The shape of the OG signal in time domain is similar to that shown in Fig. 2. Figure 4 shows that we can expect appreciable ionization of lithium vapor not only at $2p \rightarrow 4d$ resonance but over the whole range of blue-green wavelengths.

B. $2s \rightarrow 3d$ two-photon resonance

Absorption of the 639.1 nm photons is depicted in Fig. 3(b). In order to elucidate this case, LIF spectra upon the excitation by 639.1 nm laser light are taken at different lithium densities. The LIF spectra show both atomic and molecular emission. The strongest line emission comes from the $3d \rightarrow 2p$ transition. The emission from higher s and d states in a lithium atom is also present. It can be assumed that those levels are populated as a result of the recombination of lithium ions. A single rovibrational molecular level in the $Li_2\ A\,^1\Sigma_u^+$ electronic state is excited simultaneously with the two-photon resonant $3d$ state in Li. The relevant vibrational and rotational numbers are found to be $X(v''=0, J''=15) \rightarrow A(v'=7, J'=16)$ [26]. The excitation rate to the $Li(3d)$ state decreases due to this coincidence. Ionization can occur through three-photon absorption (two-photon resonant):

$$Li(2s) + 2h\nu_{639} \rightarrow Li(3d), \tag{8}$$

$$Li(3d) + h\nu_{639} \rightarrow Li^+ + e^-, \tag{9}$$

or by collisional and associative ionization from two atoms in the $3d$ level [27]:

$$Li(3d) + Li(3d) \rightarrow Li^+ + Li(2s) + e^-, \tag{10}$$

$$Li(3d) + Li(3d) \rightarrow Li_2^+ + e^-. \tag{11}$$

The OG excitation spectrum in the vicinity of the TP resonance at $2s \rightarrow 3d$ is shown in Fig. 5. The spectrum is taken at a discharge current of 30 mA and a lithium number density of 5.7×10^{15} cm^{-3}. It shows a narrow profile and does not show any enhancement at the nearby molecular transition (compare with Fig. 4 of Ref. [26]). The conclusion that can

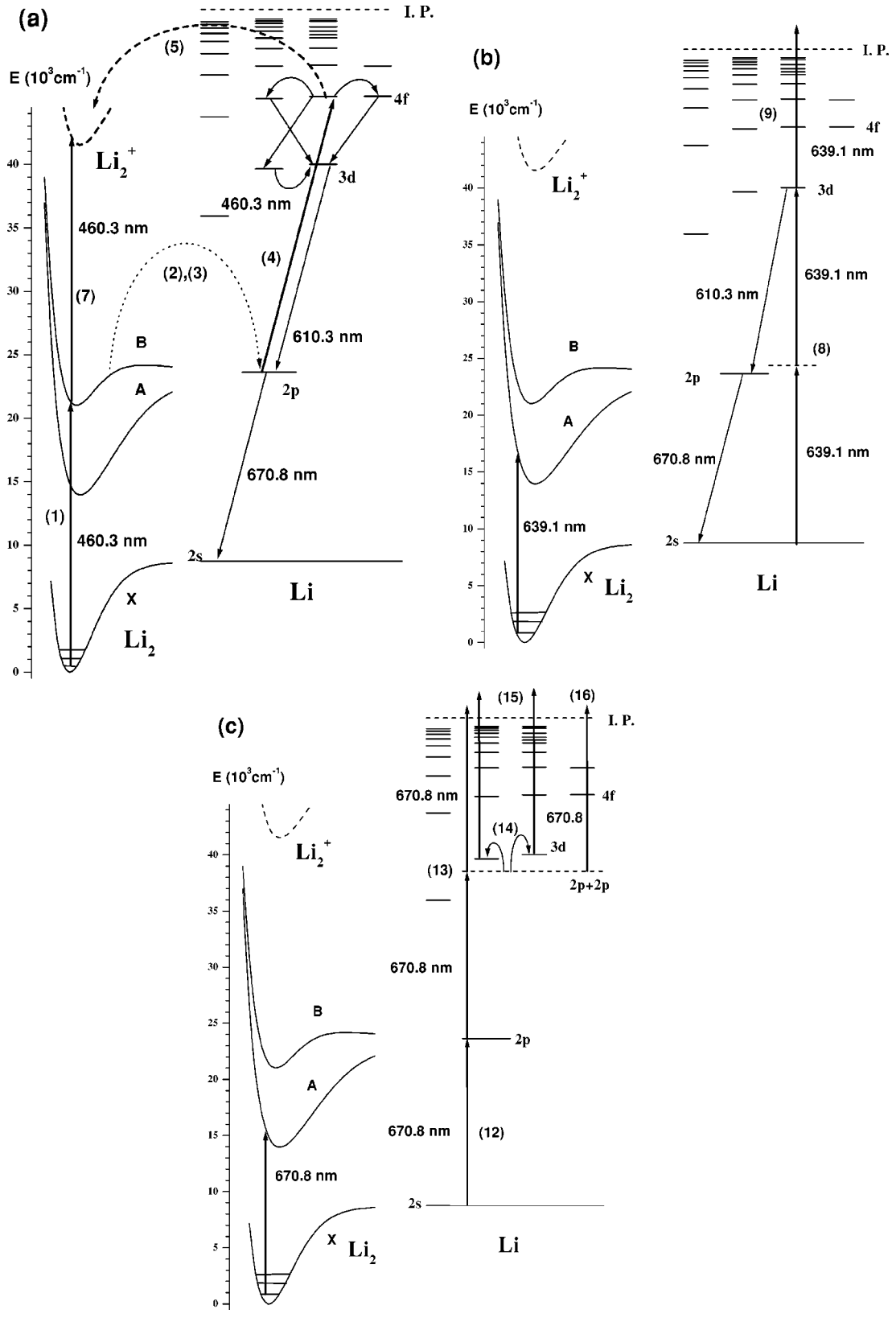

FIG. 3. Partial term diagram of lithium atom and lithium dimer in the case of (a) QR excitation at 460.3 nm. Radiative paths are indicated by straight arrows; collisional redistribution of population among 3*l* and 4*l* levels are indicated by solid curved arrows. Dimer to atom energy transfer is indicated by a dotted arrow and associative ionization by a dashed arrow. Numbers in parentheses represent processes described in the text. (b) TPR excitation at 639.1 nm. (c) FR excitation at 670.8 nm. I.P. denotes the ionization potential.

TABLE I. The most probable processes leading to the ionization of lithium vapor upon the excitation by 670.8 nm, 639.1 nm, or 460.3 nm. The total number of absorbed photons is given in parentheses.

Quasiresonant excitation		
	(1) $Li_2(X)+h\nu_{460}\rightarrow Li_2(B)$	
(2) $Li_2(B)+M\rightarrow Li(2p)+Li(2s)+M$		
(3) $Li_2(B)+Li(2s)\rightarrow Li_2(X)+Li(2p)$		
(4) $Li(2p)+h\nu_{460}\rightarrow Li(4d)$		(7) $Li_2(B)+h\nu_{460}\rightarrow Li_2^+ + e^-$ $(2ph)$
(5) $Li(4d)+Li(2s)\rightarrow Li_2^+ + e^-$ $(2ph)$		
(6) $Li(4d)+h\nu_{460}\rightarrow Li^+ + e^-$ $(3ph)$		
Two-photon excitation		
	(8) $Li(2s)+2h\nu_{639}\rightarrow Li(3d)$	
		(10) $Li(3d)+Li(3d)\rightarrow Li^+ + Li(2s)+e^-$ $(4ph)$
(9) $Li(3d)+h\nu_{639}\rightarrow Li^+ + e^-$ $(3ph)$		
		(11) $Li(3d)+Li(3d)\rightarrow Li_2^+ + e^-$ $(4ph)$
Resonant excitation		
	(12) $Li(2s)+h\nu_{670}\rightarrow Li(2p)$	
	(14) $Li(2p)+Li(2p)\rightarrow Li(3d,3p)+Li(2s)$	
(13) $Li(2p)+2h\nu_{670}\rightarrow Li^+ + e^-$ $(3ph)$		(16) $Li(2p)+Li(2p)+h\nu_{670}\rightarrow Li(2s)+Li^+ + e^-$ $(3ph)$
	(15) $Li(3d,3p)+h\nu_{670}\rightarrow Li^+ + e^-$ $(3ph)$	

be drawn is that the molecular channel does not contribute to ionization at our experimental conditions. The nonzero baseline is a result of a weak multiphoton ionization that is present over the whole wavelength region under consideration. Both LIF and OG excitation spectra show a distinct resonance at 639.1 nm in contrast to QR excitation around 460.3 nm.

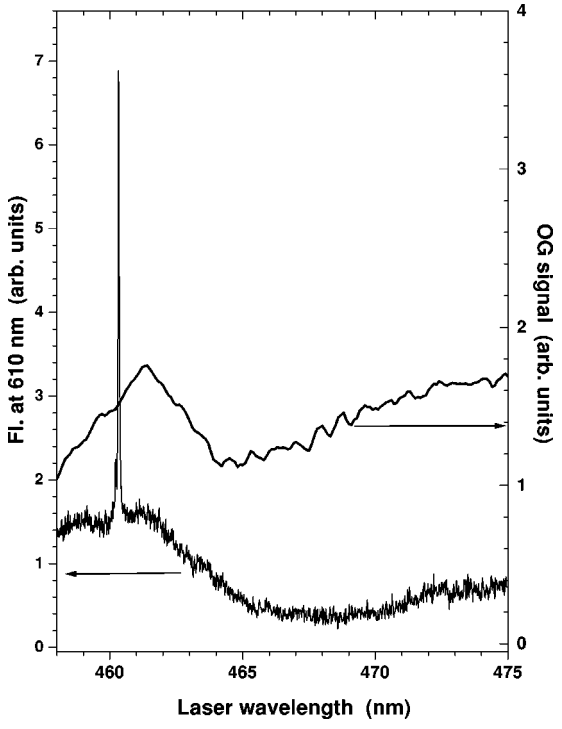

FIG. 4. The excitation spectrum of the $3d\rightarrow 2p$ transition at 610.3 nm upon scanning the laser in the wavelength interval from 458 nm to 475 nm (lower line). Excitation OG signal at 30 mA current in the same interval (upper line). Lithium number density is 1.2×10^{15} cm^{-3}.

C. $2s\rightarrow 2p$ resonance

Various absorption channels in the case of FR excitation are shown in Fig. 3(c). After the absorption of a resonant photon,

$$Li(2s)+h\nu_{670}\rightarrow Li(2p), \tag{12}$$

ions can be created by following paths. The first is a two-photon ionization of the $2p$ level:

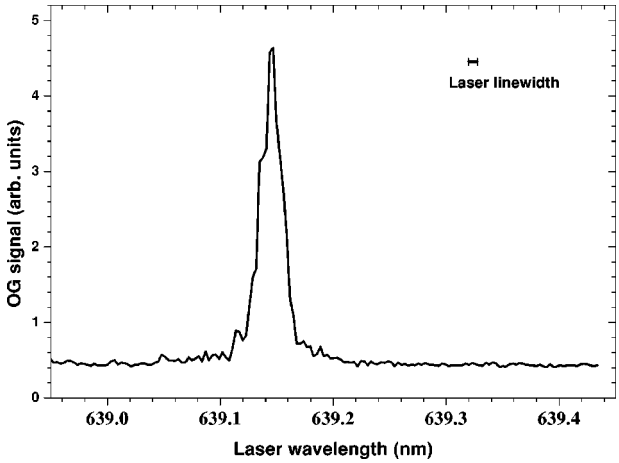

FIG. 5. OG excitation spectrum in the vicinity of the two-photon resonance at $2s\rightarrow 3d$ in lithium. Lithium number density is 5.7×10^{15} cm^{-3}.

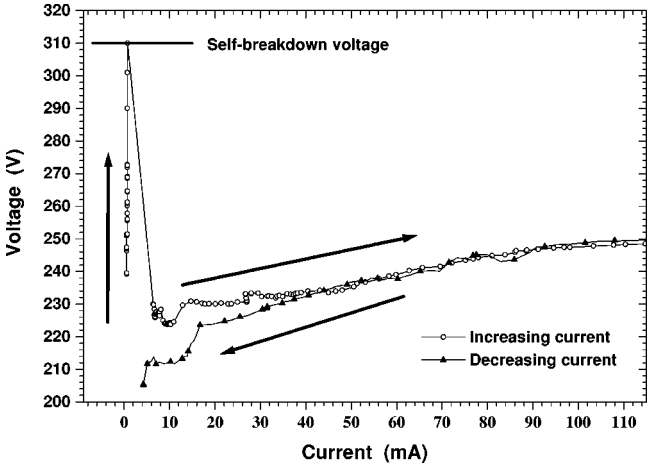

FIG. 6. A voltage versus current characteristics of the lithium glow discharge for a case of rising current and lowering current. Lithium number density is 10^{14} cm^{-3}.

$$\mathrm{Li}(2p)+2h\nu_{670}\rightarrow \mathrm{Li}^{+}+e^{-}. \tag{13}$$

The second path is energy pooling to the $3d$ or $3p$ level followed by photoionization:

$$\mathrm{Li}(2p)+\mathrm{Li}(2p)\rightarrow \mathrm{Li}(3d,3p)+\mathrm{Li}(2s), \tag{14}$$

$$\mathrm{Li}(3d,3p)+h\nu_{670}\rightarrow \mathrm{Li}^{+}+e^{-}. \tag{15}$$

The third one is radiation-assisted Penning ionization:

$$\mathrm{Li}(2p)+\mathrm{Li}(2p)+h\nu_{670}\rightarrow \mathrm{Li}(2s)+\mathrm{Li}^{+}+e^{-}. \tag{16}$$

Recently excitation of lithium vapor at 670.8 nm has been studied in relation to the energy pooling collisions [process (14)] [28]. The effective lifetimes of about 5 μs and 1 μs are measured for $2p$ and $3d$ levels, respectively, at a lithium number density of 10^{14} cm^{-3} and a laser pulse energy of about 1 mJ [29]. The radiation trapping plays an important role in defining spatial properties for the preionization of the discharge and influences the effective radiation rates. This offers a possibility for subsequent radiative ionization of $2p$, $3p$, and $3d$ levels with 670.8 nm photons from the same laser pulse or radiation-assisted Penning ionization [30].

IV. LASER IGNITION OF THE DISCHARGE

A measured voltage versus current characteristics of the glow discharge at lithium density of 10^{14} cm^{-3} is shown in Fig. 6. A hysteresis can be seen depending on whether the current through the discharge is increasing or decreasing. The drop of the voltage just after ignition can be explained by the change in electron mobility [31]. Before the breakdown, electrons freely diffuse towards the walls. After the breakdown, the diffusion is ambipolar so the loss of electrons is slower. Thus the interelectrode electric field, which governs the ionization rate, decreases in order to balance ionization and charge losses.

The laser ignition experiment consists of tuning the laser light in one of the resonances while the voltage between

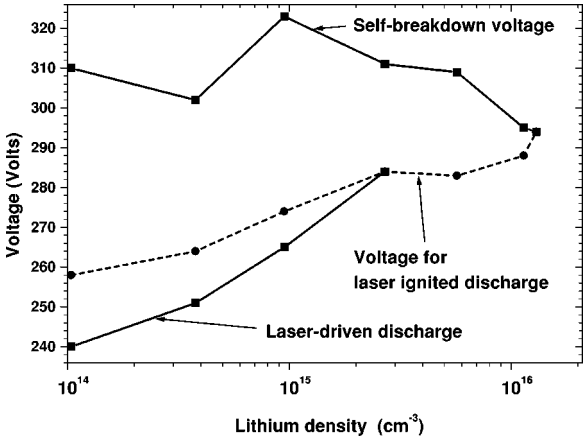

FIG. 7. Plot of voltage versus lithium number density for laser ignition of the discharge by TP resonant, $2s\rightarrow 3d$ laser pulses. The upper line represents the breakdown voltage. The middle line represents minimum voltage necessary for laser-assisted ignition of a self-sustained discharge. The area between the middle and the lower line represents the region where the laser-driven discharge can be obtained.

electrodes is below the self-breakdown voltage. A low degree ionization is created due to the relatively short duration and a modest energy of the laser pulse, but in the presence of a static electric field, free charges accelerate and create additional ionization and trigger the discharge. The difference between the self-breakdown voltage and the applied voltage could be defined as a measure of laser ignition ability. The larger this difference is, the larger is the laser ignition ability.

At lower voltage level it is possible to get an operation regime in which the discharge turns on and off with each laser pulse. We call that laser-driven discharge. When the slightly higher voltage level is set, after laser-assisted ignition the discharge is self-sustained. At lithium number densities up to 10^{15} cm^{-3}, the discharge glows in a diffuse mode, i.e., the glow fills the whole cross section of the HPO even at small current values. At higher densities, the glow is restricted to the axial region–constricted mode. This is consistent with the previous observations of the plasma column constriction in lithium glow discharges [32].

It is possible to ignite the discharge by the laser light over a broad spectral region around the quasiresonant line at 460.8 nm for lithium number density from 10^{14} to 10^{16} cm^{-3}. There is no significant increase in laser ignition ability at the position of the quasiresonance. That is consistent with the OG measurement shown in Fig. 4. It can be concluded that at these conditions (laser pulse energy and duration, lithium number density) the QR excitation $2p\rightarrow 4d$ [processes (1)–(6)] does not contribute significantly to the ionization of the vapor compared to the Li_2 ionization.

Laser ignition of the discharge by the TPR, $2s\rightarrow 3d$, laser pulse is very efficient at lower lithium number densities, but decreases towards higher lithium number densities. Figure 7 shows the regions of laser-driven and laser-ignited discharge in the voltage versus Li number density diagram. The self-breakdown voltages for that region are also shown in the picture. The laser-driven discharge region is limited to lower

lithium number densities. In these measurements the laser repetition is 1 Hz and the wavelength is at the exact position of the TPR. At the lithium number density of 1.3×10^{16} cm^{-3} and higher, the laser pulse could not induce the breakdown below the self-breakdown voltage. The probable reason for the decrease of laser ignition ability towards higher densities is the increase in $X\,^1\Sigma_g^+ \rightarrow A\,^1\Sigma_u^+$ molecular absorption.

Laser ignition of the discharge by the resonant $2s \rightarrow 2p$ pulse at 670.8 nm exhibits similar characteristics to the case of 639.1 nm excitation. A difference is that the decrease of laser ignition ability towards higher densities is more pronounced than in the case of two-photon excitation, owing to the strong absorption of the resonance line by the dense vapor.

V. CONCLUSION

We have demonstrated laser-ignited and laser-driven discharge in lithium vapor maintained within a heat-pipe oven. Among various excitation schemes, the TPR excitation at 639.1 nm is found to produce the most clear wavelength-selective effects.

We observed two regimes for laser ignition. The first is when the discharge was sustained after the initial ignition, and the second denotes a stable plasma discharge only in the presence of the resonant laser photons. Lithium number densities of about 10^{14} cm^{-3} are found to be best suited for laser ignition of the discharge.

Similar studies could be extended to other alkali-metal systems, or intermetallic systems such as LiCd or NaCd. A very efficient energy transfer from the Li($3d$) level to cadmium metastable levels offers the possibility of improved laser ignition in lithium-cadmium vapor mixture [33].

ACKNOWLEDGMENTS

This work was financially supported by the Ministry of Science and Technology of the Republic of Croatia and by US-HR Joint Board Project No. JF 151. Fruitful discussions with J. T. Bahns and W. C. Stwalley are gratefully acknowledged.

[1] B. Barbieri, N. Beverini, and A. Sasso, Rev. Mod. Phys. **62**, 603 (1990).
[2] J.T. Bahns, C.C. Tsai, B. Ji, J.T. Kim, G. Zhao, W.C. Stwalley, J.C. Bloch, and R.W. Field, J. Mol. Spectrosc. **186**, 222 (1997).
[3] A. Von Engel, *Ionized Gases* (Clarendon Press, Oxford, 1965).
[4] T.B. Lucatorto and T.J. McIlrath, Appl. Opt. **19**, 3948 (1980).
[5] T.B. Lucatorto and T.J. McIlrath, Phys. Rev. Lett. **37**, 428 (1976).
[6] A.C. Tam and W. Happer, Opt. Commun. **21**, 403 (1977).
[7] A.C. Tam, J. Appl. Phys. **51**, 4682 (1980).
[8] D. Veža and C.J. Sansonetti, Z. Phys. D: At., Mol. Clusters **22**, 463 (1992).
[9] J. T. Bahns, M. Koch, and W. C. Stwalley, in *Physics of Ionized Gases*, edited by L. Tanović, N. Konjević, and N. Tanović (Nova Science Publishers, Commack, NY, 1989).
[10] W.C. Stwalley and J.T. Bahns, Laser Part. Beams **11**, 185 (1993).
[11] R.M. Measures, J. Appl. Phys. **7**, 2673 (1977).
[12] R.M. Measures and P.G. Cardinal, Phys. Rev. A **23**, 804 (1981).
[13] T. Stacewicz and J. Krasinski, Opt. Commun. **39**, 35 (1981).
[14] T. Stacewicz and G. Topulos, Phys. Scr. **38**, 560 (1988).
[15] P. Bicchi, La Rivista del Nuovo Cimento **20**, 1 (1997).
[16] J. T. Bahns, Ph. D. thesis, University of Iowa, 1983.
[17] G. Pichler, S. Milošević, D. Veža, and R. Beuc, J. Phys. B **16**, 4619 (1983).
[18] H. Tamura, J. Mogi, K. Horioka, and K. Kasuya, Jpn. J. Appl. Phys., Part 2 **22**, L417 (1983).
[19] M. Hijikawa, H. Tamura, H. Arishima, K. Horioka, and K. Kasuya, Appl. Phys. Lett. **45**, 234 (1984).
[20] H. Tamura, K. Horioka, and K. Kasuya, J. Appl. Phys. **59**, 3722 (1986).
[21] H. Skenderović, T. Ban, and G. Pichler, J. Phys. D **33**, 396 (2000).
[22] A.N. Nesmeyanov, *Vapor Pressure of the Elements* (Academic Press, New York, 1963).
[23] Short movie files of laser-assisted ignition of the discharge are located at http://www.ifs.hr/~hrvoje/mpgs.html
[24] H-K. Chung, K. Kirby, and J.F. Babb, Phys. Rev. A **60**, 2002 (1999).
[25] J. Lahiri and S.T. Manson, Phys. Rev. A **48**, 3674 (1993).
[26] I. Labazan and S. Milošević, Eur. Phys. J. D **8**, 41 (2000).
[27] M.W. McGeoch, R.E. Schlier, and G.K. Chawla, Phys. Rev. Lett. **61**, 2088 (1988).
[28] Ch. He and R.A. Bernheim, Chem. Phys. Lett. **190**, 494 (1992).
[29] I. Labazan and S. Milošević (unpublished).
[30] S. Geltman, J. Phys. B **10**, 3057 (1977).
[31] Y.P. Raizer, *Gas Discharge Physics* (Springer Verlag, Berlin, 1997).
[32] H. Skenderović, T. Ban, and G. Pichler, Opt. Commun. **161**, 217 (1999).
[33] D. Azinović, I. Labazan, S. Milošević, and G. Pichler, Opt. Commun. **183**, 425 (2000).